J Appl Electrochem (2009) 39:31–38
DOI 10.1007/s10800-008-9635-y

ORIGINAL PAPER

Influence of the particle size on the mechanical and electrochemical behaviour of micro- and nano-nickel matrix composite coatings

C. Zanella · M. Lekka · P. L. Bonora

Received: 28 November 2007 / Accepted: 4 July 2008 / Published online: 18 July 2008

Abstract The aim of this work is the production and characterization of composite nickel matrix electrodeposits. Pure nickel and composite nickel matrix deposits containing either micro- or nano-particles of silicon carbide were prepared using a Watts type bath. The electrodeposition was carried out under both direct and pulse current conditions at different frequencies. With the same quantity of powder in the bath, the embedded micro-powder content is about 25–30%w while the nano-powder content is always less than 1%w. The mechanical properties of the nano-composites increases despite the low ceramic content. SEM micrographs of the microstructure and XRD-line profile analysis show that the presence of ceramic powder in both baths changes the crystallisation process leading to enhanced mechanical properties even at ceramic contents less than 1%, as in the nano-composite case. The presence of the ceramic phase and changes in the microstructure both decrease the mass loss during abrasion by up to 70% for micro-composites and 45% for nano-composites.

Keywords SiC · Nano-particles · Codeposition · Nickel · Pulse current

1 Introduction

Composite coatings consist of a metal or alloy matrix containing a dispersion of second phase particles. These particles are generally oxide or carbide powders such as Al_2O_3, SiC, TiO_2, SiO_2 and diamond, or solid lubricants like PTFE, graphite and MoS_2 to improve wear resistance or reduce friction [1–4]. The electrocodeposition of ceramic particles for the production of metal matrix composite coatings is a research domain of wide interest as these coating can be used for a large field of industrial applications especially in cases where high abrasive and protective properties are required. Micro-sized particles are particularly used in order to increase wear-abrasion resistance. Ni–SiC composites have been studied extensively [3–10] and commercialised successfully for the protection of mechanical parts under friction, due to their higher wear resistance. The use of micro-particles in composite galvanic coatings gives well-known improvement in the features of the surface layers. However, they also introduce some negative aspects which might be overcome by the use of nano-particles [11].

The use of nano-particles should reduce the problem of defect creation, such as voids among the particle–matrix interface. Furthermore the codeposition of a sufficient amount of non-agglomerated particles should lead to production of harder and more resistant coatings [4–6, 8–12]. Nano-composite coatings have been studied increasingly in the last 10 years, but the results are often contradictory and inconsistent and they are therefore difficult to compare with micro-composites [13, 14]. Moreover, studies have focused more on microstructural changes than on changes in properties that the nano-powders induce. Most research groups have studied either the mechanical or the protective properties of the composite coatings and not both aspects [5, 15]. Therefore it is important to carry out a complete characterization of composite coatings, testing both electrochemical and mechanical behaviour in order to quantify in a consistent way both wear and corrosion resistance.

The aim of this work is the codeposition of micro- and nano-SiC particles from nickel Watts baths using the same

C. Zanella (✉) · M. Lekka · P. L. Bonora
DIMTI, laboratorio di anticorrosione, Università di Trento,
via Mesiano 77, 38050 Trento, Italy
e-mail: caterina.zanella@ing.unitn.it

process parameters and the study of the influence of ceramic powder particle size on the electrodeposit properties.

2 Experimental

Three main groups of samples were prepared: samples coated with pure nickel deposits, samples coated with micro- and nano-Ni–SiC composite deposits. The plating solution used was a slightly modified Watts type nickel bath in which 20 g l^{-1} of SiC particles with a mean diameter of either 5 μm or 20 nm were added in order to produce the composite coatings. The composition of the plating bath and the electrodeposition parameters are given in Table 1.

In order to create stable suspensions of the ceramic powders the baths were treated by ultrasound for 30 min and mechanically stirred for 24 h before use. Furthermore, the bath was maintained under mechanical stirring during deposition (200 rpm). The substrate was 25 cm^2 low carbon steel plates. Galvanostatic deposition was carried out under both direct (DC) and pulse current (PC) conditions. The pulse current condition was used in order to produce more compact deposits [16]; it had a square form and a duty cycle of 50% and the frequencies used were 0.01, 0.1 and 1 Hz. The minimum current density was 0 while the maximum current density was maintained at 2 A dm^{-1} in order to better compare the specimens with those produced under direct current.

The coating thickness of all types of Ni-matrix deposits was 20 μm except the ones used for the abrasion resistance test. For this test specimens with 60 μm deposit were produced.

The surface morphology and microstructure of the deposits was examined by Low Vacuum Scanning Electron Microscopy (LV–SEM) and the amount of codeposited SiC particles was calculated from EDXS spectra by means of an average value of five measurements on two different specimens. The samples were also observed in cross-section after polishing and etching with a solution based on lactic acid for 4 min in order to study by LV–SEM the vertical growth of deposits grains.

X-ray diffraction and Line Profile Analysis (LPA) using the Williamson–Hall model [16] were performed to evaluate the mean crystal domain size by the Scherrer equation [17].

Microhardness measurements were carried out on three different samples for each type of deposit using a Vickers microhardness tester and applying a load of 0.1 N for 10 s on the cross-section to avoid the influence of the substrate.

The abrasion resistance of the coatings was determined by a Taber Abraser (model 5131); the wheels used were CS10 type with an additional weight of 1 kg on each wheel. Every 500 cycles the test was interrupted the wheels were cleaned and the specimens weighed. The abrasion resistance is expressed by the mass loss.

The protective properties of the coating were evaluated by the study of potentiodynamic curves in sulphuric acid solution at pH 2.5. The measurements were carried out in a three-electrode system: the potential scanning ranged from −200 mV vs. Open Circuit Potential (OCP) to 1.1 V vs. Ag/AgCl and the scan rate was 0.2 mV s^{-1}. Three potentiodynamic curves for each type of deposit were obtained on different specimens.

Table 1 Plating bath composition and deposition parameters

	Concentration (g l^{-1})
Plating solution composition	
$NiSO_4$	240
$NiCl_2$	45
H_3BO_3	30
$CH_3(CH_2)_{11}OSO_3Na$	2
SiC powder	20
Electrodeposition parameters	
pH	4.5
Temperature	45 °C
Current density	2 A dm^{-2}
Anode	Pure nickel
Substrate	Low carbon steel

3 Results and discussion

3.1 Microstructure and SiC content

The microstructure of the deposits was studied both on the surface and across a cross-section by LV–SEM. Representative surface micrographs of pure, micro- and nano-composites 20 μm thick are presented in Figs. 1–3. The surfaces of all pure nickel specimens show pyramidal grains. The application of pulse current leads to a slight grain refinement. The surface of the deposits produced under PC shows smaller pyramidal grains which form round aggregates.

The micro-composite deposits produced both under DC and PC present a very rough surface due to the high amount of partially embedded particles.

By increasing the deposits thickness (60 μm) (Fig. 4) the surface of the micro-composite coatings is almost particle-free and therefore a comparison between the different coatings is possible. In the pure nickel coatings the main grain size increases with increase in deposit thickness (Fig. 4a) maintaining a regular pyramidal structure. The micro-composite coatings have a finer microstructure

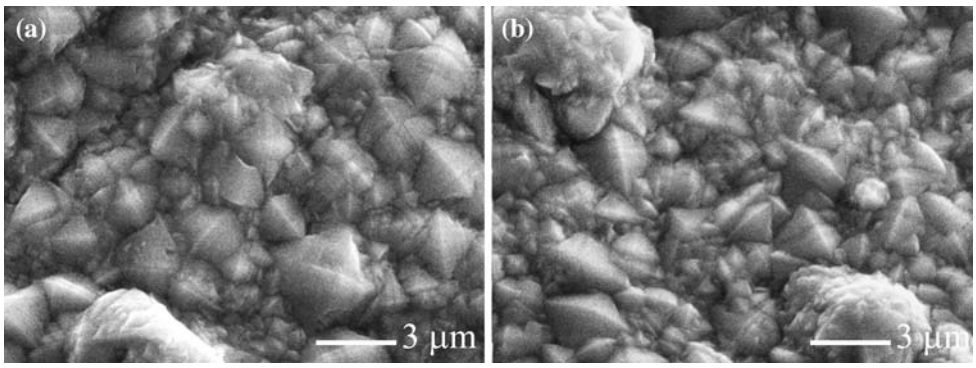

Fig. 1 Pure nickel obtained under direct current (**a**) and pulse current at 1 Hz (**b**)

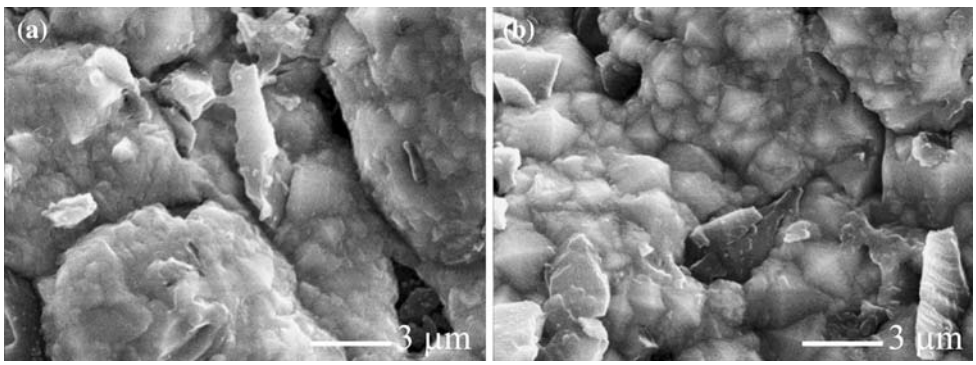

Fig 2 Micro-composite nickel obtained under direct current (**a**) and pulse current at 1 Hz (**b**)

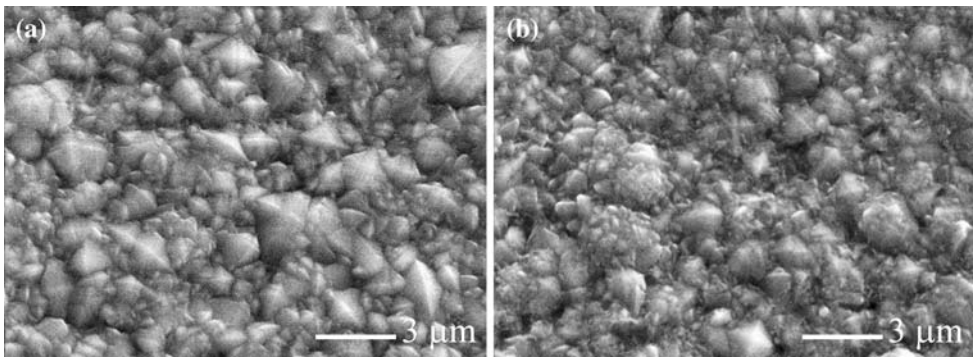

Fig. 3 Nano-composite nickel obtained under direct current (**a**) and pulse current at 1 Hz (**b**)

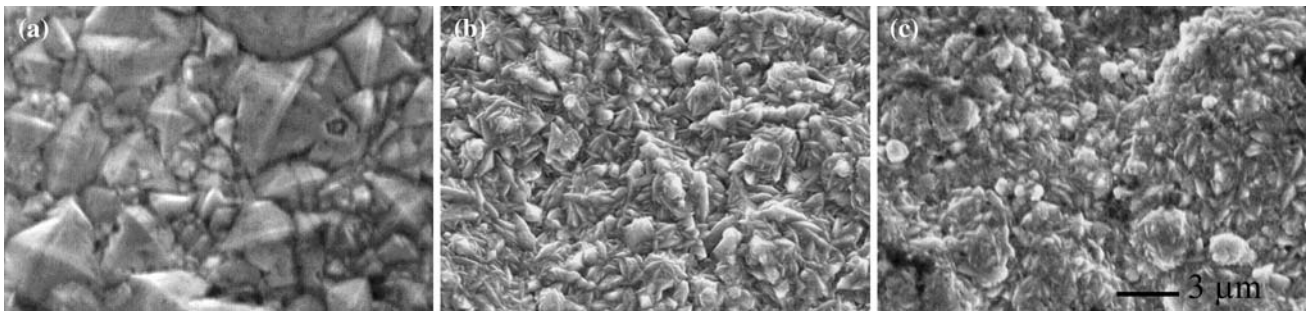

Fig. 4 Microstructure of coatings deposited under pulse current at 1 Hz with 60 μm thickness, (**a**) pure nickel, (**b**) micro-composite nickel, (**c**) nano-composite nickel

compared to pure nickel only. Regarding the nano-composite coatings, the microstructure is very fine in both 20 and 60 μm thick samples. The grains size does not increase with increasing layer thickness and is finer as compared to pure and micro-composite nickel under both DC and PC conditions.

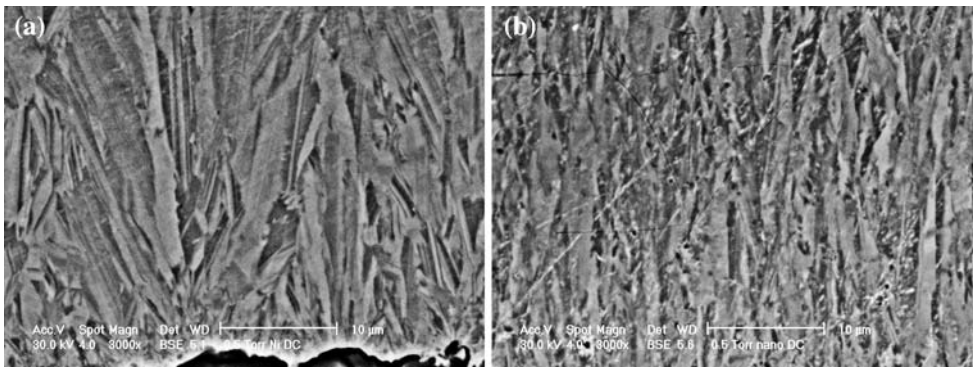

Fig. 5 Etched cross-section microstructure of pure nickel coatings deposited under direct current (**a**) and pulse current at 1 Hz (**b**) with 60 μm thickness

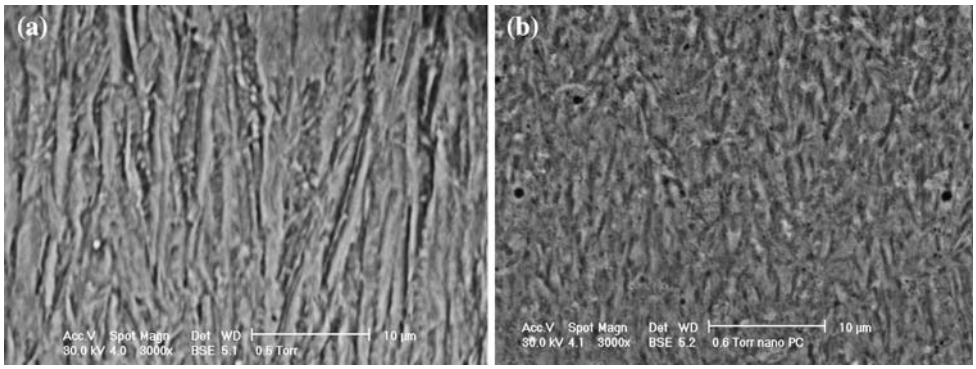

Fig. 6 Etched cross-section microstructure of nano-composite nickel coatings deposited under direct current (**a**) and pulse current at 1 Hz (**b**) with 60 μm thickness

The samples produced under PC at 1 Hz (Figs. 3b and 4c) show the finest microstructure. The grains are smaller than 1 μm and some globular grain-agglomerates are visible on the surface.

The observation of the etched cross-section of the specimens clearly shows the influence of PC application on the vertical growth of the grains. Pure nickel samples under direct current conditions (Fig. 5a) show a vertical columnar growth typical for these deposits. The columns are 2–4 μm width and the length depends on the layer thickness. The application of a pulse current decreases both the width and the length of the columns and some very small grains are visible between columns. In the case of micro-composite deposits the metallographic etchants preferentially attack the interface between the micro-particles and the matrix leading to their detachment. The nano-composite samples (Fig. 6a) deposited under direct current conditions also show vertical columnar grains, but the columns are narrower compared to pure nickel structure and their length is about 10 μm. The specimens produced with pulse current at 1 Hz (Fig. 6b) do not show any vertical growth. The microstructure is formed by globular grains with a mean dimension of about 1 μm. These observations show that the presence of a ceramic powder limits the grain growth leading to a finer microstructure. The use of PC (more evident at 1 Hz) and the codeposition of nano-powder lead to further grain refinement and thus to a drastic change in microstructure. As a consequence, better electrochemical and mechanical properties of the nano-composite coating are expected.

Table 2 SiC weight fraction in composite coatings

SiC $\%_w$	Micro-composite coatings	Nano-composite coatings
Direct current	21 ± 2	0.6
0.01 Hz	26 ± 3	0.5
0.1 Hz	36 ± 2	0.5
1 Hz	24 ± 4	0.9

Using an EDXS probe during SEM observation it was possible to evaluate the fraction of codeposited SiC. The results are summarized in Table 2.

The content of codeposited SiC nano-particles is very low, close to the resolution limit of this analysis. No comparison is therefore possible between different coatings, even if at 1 Hz a slight increase in SiC content is observed. Conversely, when a micro-powder of SiC is added the amount of ceramic incorporation is high and depends on the deposition parameters. The use of a pulse current increases the ceramic content from 21 to a maximum of 36% w for specimens deposited at 0.1 Hz.

3.2 LPA of X-ray diffraction

Line profile analyses of X-ray diffraction spectra were performed using the Williamson–Hall model and the Scherrer equation was applied to peak broadening in order to correlate them to crystal domain size. The results are reported in Table 3. It is clear that the presence of a

Table 3 Evaluation using the Williamson–Hall model of crystal size (nm) of different coatings

	Pure nickel	Micro-composite nickel	Nano-composite nickel
Direct current	94 ± 3	58 ± 6	59 ± 3
0.01 Hz	100 ± 16	56 ± 6	59 ± 4
0.1 Hz	92 ± 4	56 ± 6	61 ± 1
1 Hz	80 ± 9	62 ± 6	51 ± 4

ceramic phase decreases the crystal domain size from about 100 to 60 nm. The crystal domain size determined by this analysis is different to the grain size observed by LV–SEM. Crystal domains are limited by crystal defects and internal stresses and therefore a single grain can contain more crystal domains. Parameters like current condition and ceramic particle dimension do not affect the crystal domain size but have a strong effect on the grain size.

3.3 Microhardness

The results obtained measuring microhardness in the cross-sections of samples are reported in Fig. 7. The hardness of pure nickel coatings is about 280 HV and is not noticeably influenced by current condition. The micro-composite coatings present the highest microhardness due to the high amount of codeposited ceramic powder; the error bar in this case is very large and this is due to the heterogeneity of the layer which contains particles comparable in size to the indenter. Therefore the variations in the obtained values could not be correlated to the codeposited SiC amount. The presence of the nano-particles at the grain boundaries as well as the increase in number grain boundaries causes slight modification to the microhardness due to the strain hardening effect. Indeed the nano-composite deposit produced under PC at 1 Hz which present the finest microstructure (Fig. 6b) also has a microhardness value comparable to those of micro-composites.

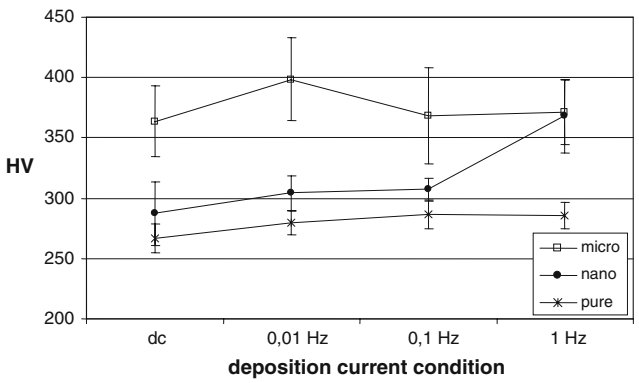

Fig. 7 Vickers 001 microhardness values

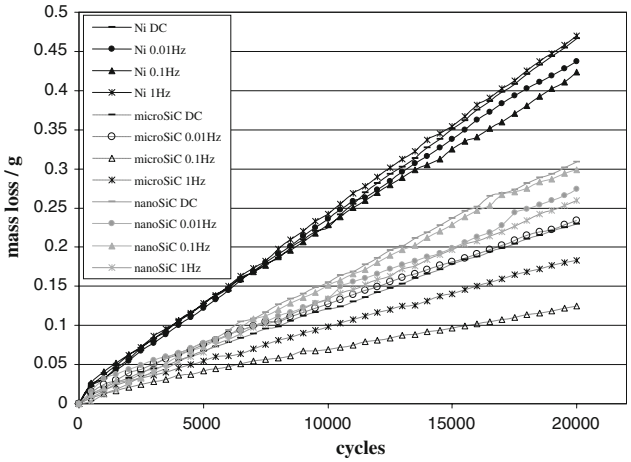

Fig. 8 Mass loss during abrasion test

3.4 Abrasion resistance

The abrasion resistance presented in Fig. 8 is expressed by the mass loss calculated by weighing the samples every 500 cycles. In this test 60 μm thick deposits were used.

The pure nickel coatings lose about 0.45 g after 20,000 cycles and no big differences are visible between samples produced under different current conditions. The curves of mass loss indeed overlap up to 10,000 cycles and only small differences are visible after 20,000 cycles. These differences are due to the experimental error. Therefore deposition under pulse current does not improve the abrasion resistance of the nickel coatings. It is evident that both nano- and micro-composite coatings offer better resistance to abrasion than pure nickel coatings.

Regarding micro-composite deposits, the current condition has a major effect on the abrasion resistance. The curves corresponding to the deposits produced under DC and PC at 0.01 Hz are almost overlapped. The specimens produced under PC at 0.1 and 1 Hz show a decrease in mass loss after 20,000 cycles of 40 and 20% respectively. The abrasion resistance of micro-composite is strongly related to the amount of codeposited SiC. The deposit with the higher abrasion resistant is the one with the major quantity of codeposited hard phase. This fact is not in complete agreement with the values presented in the Table 2 as the result of EDXS analysis is a surface analysis and does not correspond to the whole depth of the deposit.

In the case of nano-composite coatings, the application of PC at 0.01 Hz and 1 Hz gives slightly lower mass loss at the end of the test in comparison to the samples produced under DC and PC at 0.1 Hz. However this difference is comparable to the accuracy of measurement and therefore cannot be correlated to the deposition parameters.

The abrasion resistance is strongly dependent on the size of embedded particles and much less on the applied current

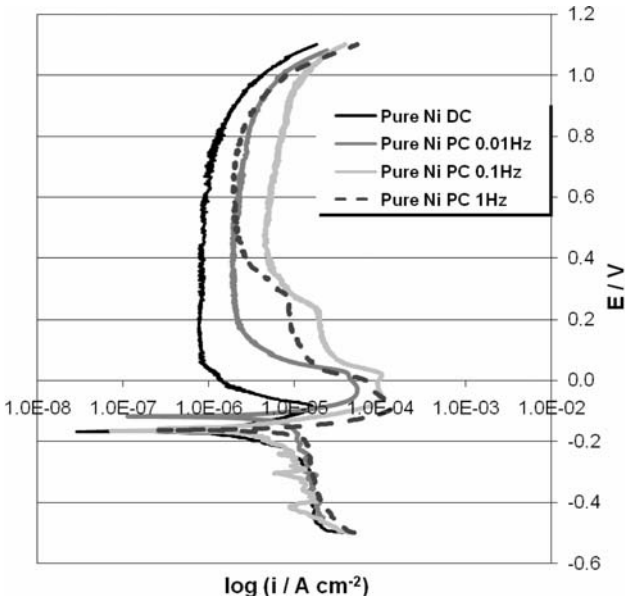

Fig. 9 Potentiodynamic curves of pure nickel coatings obtained under different current conditions

condition. The micro-composite deposits present the highest abrasion resistance while the nano-composite ones have an intermediate behaviour. It is noticeable that the nano-composite deposits produced under PC at 1 Hz have a similar abrasion resistance as the micro-composite deposits under DC and PC at 0.01 Hz even though they contain a much lower amount of SiC. Thus the microstructure modification produced by the incorporation of nano-particles leads to a drastic increase in abrasion resistance.

3.5 Potentiodynamic curves

Potentiodynamic curves were obtained from a sulphuric acid solution at pH 2.5 and room temperature in order to evaluate the active–passive transition of nickel based coatings and their resistance to uniform corrosion.

All specimens showed passive behaviour even though, according to the Pourbaix diagram, nickel should not passivate at pH 2.5. The transition from active to passive behaviour is evident in all potentiodynamic curves in Figs. 9 and 10. The pure nickel deposits produced under DC show lower critical current density and lower passive current density and a more stable and wider passive zone. The deposits produced under PC have lower tendency to form a stable passive region and higher passive current densities. This behaviour may be attributed to the microstructural changes that the use of OC causes on the deposits. Indeed, the deposits having the finest microstructure and, as a consequence, more extended grain boundaries present have less tendency to create a stable passive oxide film. The grain boundaries present preferential points for corrosion attack from the acidic solution.

Concerning micro-composite coatings (Fig. 10a) there are no substantial differences between the deposits. The corrosion potential and current densities, as well as the passive current density, are equal. The differences between the nano-composite deposits (Fig. 10b) are even less evident. The active parts of the curves completely overlap and there are some differences corresponding to the formation of the passive film. The passive zone is stable and all specimens have the same passive current density and the same passive range. Indeed, the differences in the microstructure on the surface of these deposits were not as prominent as in the case of the pure and micro-composite deposits.

In Fig. 11 the curves of the tree types of deposit produced under the same current condition are reported in order to better understand the effect of particle incorporation on the corrosion resistance in acidic environment. The specimens coated with the micro-composite deposit under

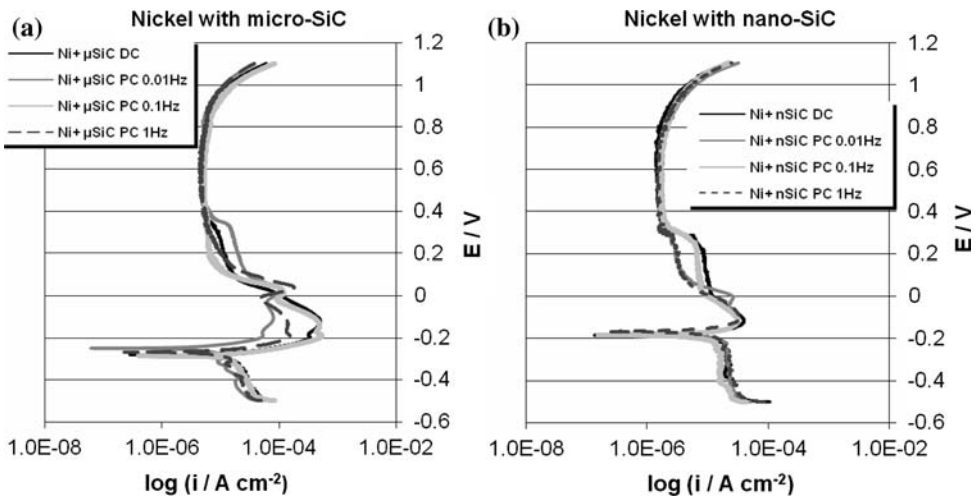

Fig. 10 Comparison between potentiodynamic curves of micro- (**a**) and nano- (**b**) composite coatings deposited under different current conditions

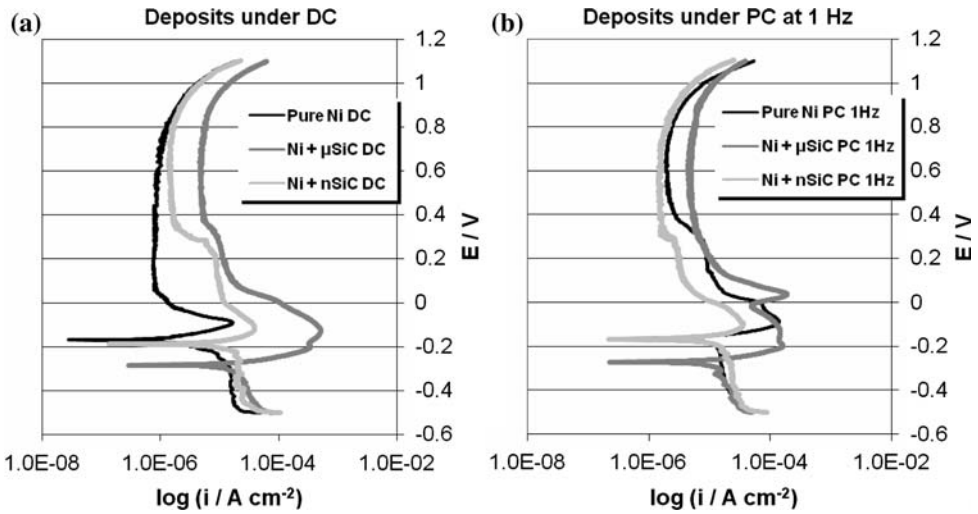

Fig. 11 Comparison between potentiodynamic curves of pure, nano- and micro-composite nickel deposited under direct current (**a**) and pulse current at 0.01 Hz (**b**)

each current condition have a lower corrosion potential and a higher corrosion current density as well as the highest passive current density. Pure and nano-composite deposits have similar corrosion potential and corrosion current densities in all cases.

4 Conclusion

The aim of this work was to study the influence of the codeposition of micro- and nano-particles of SiC in nickel matrix deposits under both direct and pulse current on microstructure and mechanical and electrochemical properties.

The use of pulse conditions in pure nickel deposits leads to a slight refinement of the microstructure but not to any significant change in the final properties of the coatings. The codeposition of the SiC micro-particles leads to a crystal domain size decrease and to grain refinement. The high amount of codeposited ceramic powder causes a significant increase in the mechanical properties; the microhardness is 100 HV higher and the abrasion resistance increases by 50–70% compared to pure nickel. The incorporation of the micro-powder causes a decrease in corrosion potential as well as an increase in corrosion and passive current density due to the weakness of the interface between matrix and particles.

The codeposition of the SiC nano-particles under both DC and PC current condition leads to a drastic grain refinement more evident at a frequency of 1 Hz. The deposits produced at this frequency have small unoriented grains. The columnar growth is inhibited by the synergism of both the interrupted electric field and the codeposition of nano-particles limiting their dimension. Therefore a slight increase in microhardness is observed for the deposits produced under DC and PC up to 0.1 Hz, while the deposits obtained at 1 Hz show a significant increase in microhardness. The nano-composite deposits produced under PC at 1 Hz show a similar abrasion resistance to the micro-composite deposits under DC and PC at 0.01 Hz even though they contain a much lower amount of SiC. The potentiodynamic curves show that nano-composite films have the same corrosion potential as well as corrosion current density as pure nickel coatings and also the passivity region is similar. The increase in the mechanical properties of micro-composites coating is due to the presence of a hard ceramic phase, while the nano-composite films owe their mechanical improvement mainly to the large microstructure changes.

Acknowledgments The authors thank the microstructures group of the Department of Material Engineering and Industrial Technologies of the University of Trento for the XRD measurements and in particular Prof. Paolo Scardi for useful discussion.

References

1. Guglielmi N (1972) J Electrochem Soc 119:1009
2. Roos JR, Celis JP, Fransaer J, Buelens C (1990) J Metals 42:60
3. Hovestad R, Janssen LJJ (1995) Rev Appl Electrochem 40:519
4. Benea L, Bonora PL, Borello R, Martelli A (2002) Wear 249:995
5. Zimmermann AF, Palumbo G, Aust KT, Erb U (2002) Mater Sci Eng A328:137
6. Hou KH, Ger MD, Wang LM (2002) Wear 253:994
7. Garcia I, Fransaer J, Celis JP (2001) Surf Coat Technol 148:171
8. Low CTJ, Willis RGA, Walsh FC (2006) Surf Coat Technol 201:371
9. Gyftou P, Stroumbouli M, Pavlatou EA, Asimidis K, Spyrellis N (2005) Electrochim Acta 50:4544
10. Lekka M, Kouloumbi N, Gajo M, Bonora PL (2005) Electrochim Acta 50:4551
11. Surender M, Balasubramanian R, Basu B (2004) Surf Coat Technol 187:93
12. Garcia I, Conde A, Langelaan G, Fransaer J, Celis JP (2003) Corros Sci 45:1173
13. Medelienè V (2002) Surf Coat Technol 154:104

14. Malfatti CF, Ferreira JZ, Santos CB, Souza BV, Fallavena EP, Vaillant S, Bonino JP (2005) Corros Sci 47:567
15. Pavlatou EA, Stroumbouli M, Gyftou P, Spyrellis N (2006) J Appl Electrochem 36:385
16. Zimmerman AF, Clark DG, Aust KT, Erb U (2002) Mater Lett 52:85
17. Williamson GK, Hall WH (1953) Acta Metall 1:22
18. Cullity (1978) Elements of X-ray diffraction, 2nd edn. Addison Wesley Publishing, London